ELECTROCHEMICAL MECHANISMS OF HYDROGEN INCORPORATION IN ELECTROLESS COPPER FILMS

BY

ANDREW MOREIRA

A thesis submitted to the

Department of Physics

Mount Allison University

in partial fulfillment of the requirements for the

Bachelor of Science degree

with Honours

April, 2019

ABSTRACT

Hydrogen incorporation in electroless copper films is a well-known source of void formation and embrittlement, which reduces the ductility of copper films and can lead to circuit failure. A non-invasive method for measuring hydrogen incorporation in electroless Cu films was utilized, and a method for driving the surface potential of the substrate is implemented. Films with rougher substrate surfaces incorporate more hydrogen, and take significantly longer to release it, than smoother surfaces of the same substrate. The stabilizer system is the fundamental driver of hydrogen incorporation into electroless Cu films. Additionally, a method for investigating the mechanism by which nickel lowers hydrogen incorporation is put forward.

ACKNOWLEDGMENTS

I would like to thank Delilah Brown showing me the ropes early on, and always being there if I needed help on a project.

I would like to thank Alexandre Leger, your friendship made those long days in the prep lab many times more bearable. I learned from your curiosity and sought to emulate your practice. I am deeply sorry for shattering your favorite beaker, I hope you can find it in your heart to forgive me.

I would like to thank my supervisor, Dr. Ralf Bruening, for your patient and methodological mentorship over the past year. I could have never completed this project without your guidance, and your attention to detail improved has improved the quality of my work immensely.

I would like to thank my parents, Melissa Ladenheim and Jamie Moreira, for their love and support throughout my undergraduate studies. I would not be where I am today without you two.

Contents

ABSTRACT i

ACKNOWLEDGMENTS ii

TABLE OF CONTENTS iii

LIST OF FIGURES iv

1 INTRODUCTION 1

2 THEORY 3

2.1 Chemistry of electroless plating 3

2.1.1 Oxidation of formaldehyde 4

2.1.2 Relation between hydrogen and Cu production 5

2.1.3 Consumption of hydroxide ions by the electrolyte 6

3 EXPERIMENT 9

3.1 Substrate Composition 9

3.2 Pretreatment of samples 10

3.3 Bath characteristics 10

3.4 Bath Maintenance 11

3.5 Measurement of hydrogen during plating 11

3.6 Addition of stabilizer component 13

3.7 Measurement of hydrogen after plating 13

3.8 Monitoring and controlling the mixed potential 14

3.9 Data Analysis 17

4 Results 20

4.1 The effect of surface roughness on hydrogen content 20

4.1.1 Measuring hydrogen incorporation 21

4.2 Stabilizer effect on hydrogen incorporation 23

4.3 Stabilizer effect on hydrogen generation 24

4.4 Stabilizer decomposition with time 25

4.5 Simulating the Ni effect with a potentiostat 26
4.5.1 Potentiostat effect on hydrogen incorporation 27
4.6 Effect of the stabilizer on the mixed potential 28

5 Discussion **30**
5.1 Substrate roughness and hydrogen incorporation 30
5.2 Stabilizer's role in hydrogen incorporation 31
5.3 Potentiostat driven surface potential 33
5.4 Mixed potential and the stability of water 34

6 Conclusion **35**

REFERENCES **37**

List of Figures

2.1 Pourbaix diagram for Cu. The green circle indicates the typical pH and electric potential of Cu plating baths. Reproduced from reference Bindra & White (1990). 7

3.1 Schematic for the setup constructed to capture gas evolved during plating. 12
3.2 Schematic of device used to indirectly measure H_2 evolution after plating. Image reproduced from Sharma et al. (2018). 13
3.3 Electrical contacts into the bath. When the mixed potential was measured, the sample and reference electrodes were detached from the circuit in Figure 3.4. The thermometer and the aeration device are also present in the bath. 15
3.4 Schematic of the potentiostat. The variable resistor is denoted by the box with the diagonal arrow running through it. 16
3.5 Picture of a sample close to the maximum area fraction. Notice the clear distinction between the Cu (light blue) and the FR4 (dark blue). 17
3.6 Image of sample after converting to black and white. This process creates a binary between area covered by H_2 and area that is not. . . 18

4.1 Average gas layer thickness, $\bar{h}$ over time for films prepared with Electroless bath type A and RA. Both desmeared and non-desmeared samples were tested. Non-desmeared data are represented in orange, desmeared data in teal. 20
4.2 The ratio between deposited Cu and incorporated hydrogen by substrate roughness for Electroless bath type B bath. 21
4.3 The ratio between deposited Cu and incorporated hydrogen by substrate roughness for Electroless bath type A bath. 22
4.4 The ratio between deposited Cu and incorporated hydrogen as a function of Ni content in the bath. Further delineations are made between baths with and without stabilizer, and between baths where the stabilizer is added after the formaldehyde. 23

4.5 Volume of hydrogen evolved during plating for 100 % stabilizer and 0 % stabilizer in Elecroless bath type C. Notice the slight delay between starting the plating and the measurement of hydrogen. 24
4.6 Volume of hydrogen evolved during plating for 100 % stabilizer solutions by volume. An active component degraded overtime, which reduced the poisoning of the surface by the stabilizer. Electrolyte: Electroless bath type C. 25
4.7 Open circuit potential of plating baths for Electroless bath type C. Notice that Ni produces a cathodic shift and also prevents the potential from becoming more positive as plating increases. 26
4.8 Potential for open circuit mixed potential vs controlled voltage trials done with a Cu substrate in a Electroless bath type C electrolyte. The initial fluctuations come from adjusting the variable resistor in order to attain a desirable voltage. 27
4.9 Potential for open circuit vs potentiostat driven (to -1.0 V) trials done a Cu-clad substrate in Electroless bath type C bath. The initial fluctuation comes from adjusting the variable resistor in order to attain a desirable voltage. 28
4.10 Mixed potential as a function of time. Notice both the wide range of potentials for baths without stabilizer and the effect that is produced when the bath is dosed up to [Ni]=800 ppm. Compare to Figure 4.7 for results with stabilizer added. 29

5.1 SEM micrograph with [Ni]=3mg/l and y=0.2. Notice how the roughness of the substrate promotes areas of the film with high thickness. Image via M. Balli, N. Baulke, and S. Heitz. Electrolyte: Electroless bath type C. Reproduced from Leger (2018). 31
5.2 Total hydrogen gas production in Electroless bath type C baths at both 0 and 100 % stabilizer. Notice little change between the two charts in total gas released, as all the change comes from the suppression of y. 32

Chapter 1

INTRODUCTION

Thin metal films are primarily manufactured through two methods, galvanic and electroless. In galvanic plating, an external current is applied to two electrodes, one anode one cathode. Oxidation occurs at the anode and the electrons flow through the wire onto the cathode, where they reduce aqueous metal ions and create a metal film on the surface. Electroless methods simplify the process by removing the external current and keeping only one electrode, the plating surface, relying instead on chemical reactions in the electrolyte to drive plating. Electroless Cu plating is an important industrial process that is used for the large-scale manufacture of printed circuit boards (PCBs). [1, 2, 3] With the proper activation process, metals such as Cu can be plated on organic substrates. Cu is an good conductor, and its low resistivity allows it to carry high currents. This technology is important as it forms the physical basis for the information and electronics-driven economies of the modern world. As a greater burden is placed on manufacturers to miniaturize circuitry, so too are the demands on the thin Cu films that form the basis for these complex electronics.

Hydrogen incorporation in Cu films is known to produce blistering and voids, and this mechanism is known to partly contribute to increased stress in the film. [4, 5] The addition of nickel has been shown to decrease film stress, hydrogen incorporation, and to counter blistering. It has also been shown that the addition of nickel produces a cathodic shift in the mixed potential of the plating surface. [6] It is currently unclear how the Ni produces this shift, whether it is a result of Ni catalyzing the decomposition of Cu hydride complexes during plating or whether if it is indirectly linked via

separate reactions on the substrate. A method for demonstrating the link, and some initial data is offered in this investigation.

The buildup of hydrogen in Cu films occurs through the intake of atomic hydrogen into the Cu lattice. The formation of voids and blisters in the films is the result of the desorption of molecular hydrogen from the film into high pressure voids, which contributes to high film stress, lower ductility, and performance. [1] The hydrogen in the Cu film congregates at voids in the film where, if the pressure is high enough, can cause blisters when the gas escapes. [2]

I would like to recognize the work that Tanu Sharma and Alex Leger have done leading up to this research. Their work provided a theoretical framework for my own, and they developed many of the analysis techniques that were used throughout this thesis. Specifically, their work on the relationship between Ni concentration and hydrogen incorporation has proved very useful to my work. My contribution surrounds the electrochemical processes that the film undergoes under the presence of nickel and stabilizer, and the influence that substrate roughness has on hydrogen incorporation. I finish with an initial test of a new technique for exploring how the surface potential of the plating surface impacts hydrogen incorporation, which provides insight into the cathodic shift in the mixed potential under the presence of Ni.

Chapter 2

THEORY

2.1 Chemistry of electroless plating

Electroless Cu plating, outlined in Chapter 1, utilizes a plating bath with formaldehyde and Cu ions to drive a plating reaction on a substrate. No external current is required, thus formaldehyde plays the role of the reducing agent to drive the reaction. The reaction proceeds as follows:

$$Cu^{2+} + 2HCHO + 4OH^- \rightarrow Cu + 2HCOO^- + H_2 \tag{2.1}$$

This reaction can also proceed without the generation of hydrogen.

$$Cu^{2+} + HCHO + 3OH^- \rightarrow Cu + HCOO^- + 2H_2O \tag{2.2}$$

The evolution of hydrogen gas during the plating process comes from the oxidation of formaldehyde on the surface of the substrate. [7] Reaction 1 is favored in Cu-rich electrodes and Reaction 2 is favored in the presence of other metals such as Pt, or Ni. [8] The relationship between hydrogen incorporation and [Ni] is developed further in Sharma et al. (2018), where they provide a quantitative measure of hydrogen released after plating by the amount of nickel content in the bath. The next three subsections concern the oxidation of formaldehyde and the reduction of Cu on the surface of the substrate. This will explain the process by which Cu is plated onto an organic substrate, how hydrogen is incorporated into the Cu lattice, and how HCHO and OH^- are consumed in the electrolyte.

2.1.1 Oxidation of formaldehyde

Consider a single molecule of formaldehyde. The formaldehyde begins the reaction through undergoing hydrolysis. This produces a methlyene glycol. [9]

$$\mathrm{HCHO} + \mathrm{H_2O} \rightarrow \mathrm{CH_2(OH)_2} \tag{2.3}$$

The methylene glycol then becomes ionized by the high pH of the plating solution. This methlyene glycol ion is then adsorbed onto the surface of the substrate. In this process, a hydrogen is removed from the methlyene glycol and is independently adsorbed onto the surface of the substrate. Molecules with the "ad" subscript denote those particles attached to the substrate surface.

$$\mathrm{CH_2(OH)_2} + \mathrm{OH^-} \rightarrow [\mathrm{CH(OH)O^-}]_{ad} + \mathrm{H}_{ad} + \mathrm{H_2O} \tag{2.4}$$

The adsorbed ion is oxidized, and this contributes the first of two electrons required to reduce $\mathrm{Cu^{2+}}$.

$$[\mathrm{CH(OH)^-}]_{ad} + \mathrm{OH^-} \rightarrow \mathrm{HCOO^-} + \mathrm{H_2O} + e^- \tag{2.5}$$

The adsorbed hydrogen, on the other hand, will undergo a substrate-dependent reaction where it is either oxidized by a hydroxide ion, combined with another adsorbed hydrogen molecule to form hydrogen gas, or incorporated into the Cu film. This is the reaction that forms the Cu seed layer, a thin layer of Cu a couple of atoms thick, upon which more Cu atoms can plate onto the surface. [8] Additionally, the presence of Ni suppresses hydrogen incorporation in Cu films. [6, 10]

$$H_{ad} + OH^- \rightarrow H_2O + e^- \tag{2.6}$$

$$2H_{ad} \rightarrow H_2 \tag{2.7}$$

2.1.2 Relation between hydrogen and Cu production

The remaining adsorbed hydrogen is incorporated into the Cu film through the formation of Cu hydride. The ratio between the hydrogen evolved after plating and Cu deposited on the film, y, is representative of the hydrogen incorporated into the film during plating.

$$Cu + yH_{ad} \rightarrow CuH_y \tag{2.8}$$

Now we can develop a model for relating x and y to Reactions (2.1) and (2.2). In Reaction (2.1), there are two hydrogen atoms generated (via one molecule of H_2) for each atom of Cu plated. In Reaction (2.2), no hydrogen atoms are generated for each Cu atom plated. Thus, the total amount of hydrogen atoms generated during should be between zero and two times the amount of Cu plated. That is, $0 \leq x + y \leq 2$, where x is the mole ratio of hydrogen generated during plating to the amount of Cu plated. To synthesize Reactions (2.1) and (2.2) into a single reaction, first take their difference, and multiply that result by $\frac{x+y}{2}$, the ratio of moles of H_2 generated to Cu plated. [11]

$$HCHO + OH^- \rightarrow HCOO^- + H_2 \tag{2.9}$$

$$\frac{x+y}{2}HCHO + \frac{x+y}{2}OH^- \rightarrow \frac{x+y}{2}HCOO^- + \frac{x+y}{2}H_2 \tag{2.10}$$

Now add this result to Reaction (2.2) to obtain the following expression

$$Cu^{2+} + (\frac{x+y}{2} + 1)HCHO + (\frac{x+y}{2} + 3)OH^- \rightarrow Cu + (1 + \frac{x+y}{2})HCOO^- + \frac{x+y}{2}H_2 \tag{2.11}$$

Incorporate Reaction (2.8) to simplify Reaction(2.11) to the following:

$$Cu^{2+} + (\frac{x+y}{2} + 1)HCHO + (\frac{x+y}{2} + 3)OH^- \rightarrow CuH_y + (1 + \frac{x+y}{2})HCOO^- + \frac{x}{2}H_2 \tag{2.12}$$

Reaction (2.12) gives an idea of the distribution of Reaction (2.1) and (2.2) during plating. This enables a distinction between which of those two equations dominate, and whether the hydrogen is incorporated into the film, or evolved during plating.

2.1.3 Consumption of hydroxide ions by the electrolyte

An important side reaction occurs in the plating bath even when Cu plating is not occurring. The Cannizzaro reaction consumes formaldehyde and hydroxide ions and outputs methanol and formate. [9]

$$HCHO + HO^- \rightarrow HCOO^- + CH^4OH \tag{2.13}$$

This has multiple effects, one of which being that methanol content in the bath is a marker of the age of the bath, as Reaction (2.13) occurs continuously in the bath. Importantly, Reaction (2.13) consumes formaldehyde that would otherwise be used to reduce the plating surface, and so this requires the periodic replenishment of formaldehyde throughout a bath's life. Additionally, it reduces the pH of the bath, as it removes OH^- and inputs H^+ via formate ions. This negatively impacts the formation of Cu(s) on the substrate surface, as shown by Figure 2.1. [12]

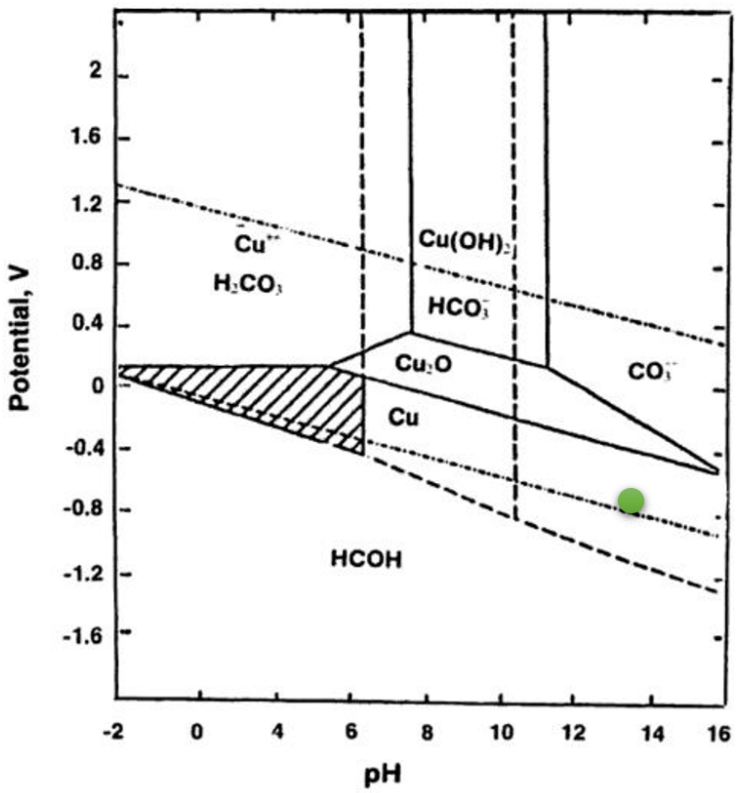

Figure 2.1: Pourbaix diagram for Cu. The green circle indicates the typical pH and electric potential of Cu plating baths. Reproduced from reference Bindra & White (1990).

A decrease of the pH, with potential held constant will make the oxidation of HCOH unfavorable, thus Reaction (2.3) will not proceed and plating will not occur. Another side reaction also lowers the pH, and occurs even when the bath is not in use. Carbon dioxide reacts with hydroxide ions accordingly to Reaction (2.14) and, given the baths are aerated, CO_2 is continuously introduced by the airflow.

$$2HO^- + CO_2 \rightarrow {CO_3}^{2-} + H_2O \tag{2.14}$$

Therefore, like formaldehyde, the OH^- content of the plating baths must be monitored

closely. Additionally we see that this reaction has the effect of reducing the pH of the bath through the consumption of hydroxide ions. In effect, the reaction adds carbonic acid, a weak acid, into the bath.

The dot-dashed lines in the diagram indicate the stability range of water. The setpoint of a standard electrolyte, shown by the green dot, at around a pH of 13.6 and a mixed potential -0.8 V, sits close to the edge of that stability range. [13] This is relevant here because Reaction (2.6), requires in principle that the the experiment stays above the dot-dashed line, i.e. it is required that water is stable.

Chapter 3

EXPERIMENT

3.1 Substrate Composition

The Cu was plated on two substrates: FR4 and Cu-plated FR4. The Cu substrate was formed by plating a very thin layer of Cu precursor on a piece of FR4. The FR4 plastic is a common organic substrate for PCBs and is the primary substrate for these experiments, unless noted otherwise. The thin Cu film pre-plated on the FR4 was used for the voltage experiments so the surface potential could be controlled instantly and would not have to wait for Cu to be plated on. The pieces of FR4 were cut into squares of roughly 25 cm^2 area, and each square was the basis for a single sample. The sheets of FR4 underwent a process of desmearing, wherein one surface was made artificially rougher. This was done to increase the effective surface area of the substrate and thus incorporate more Cu into the plating, which in theory produces thicker films.

For the controlled surface potential experiment, it was necessary that an electrical connection be established from a potentiostat to the surface of the sample immediately, so the surface potential could reach the desired voltage as quickly as possible. To do this, each piece of FR4 was plated with a thin layer of Cu, corresponding to 4 minutes submerged in a Electroless bath type C Bath. The desmeared side was marked to make sure each side remained distinguishable even after the Cu layer had been placed on top of the FR4. Measurements for the controlled surface potential experiments were done on the Cu layer plated on the desmeared side.

3.2 Pretreatment of samples

Before a sample can undergo electroless plating, it must first be activated, by a pre-treatment process that is substrate specific. That is a partially formed conducting layer must be formed on the surface of the substrate where the initial layer of Cu can form. First, the substrate is immersed in a cleaner for several minutes at 50^oC. It is then moved to a palladium solution (200mg/L Pd), where it is kept for several more minutes at 45^oC. In the final step of the process, the substrate is placed in a solution at 30^oC that reduced the Pd on the surface of the substrate. In between each step, the substrate was cleaned with tap and then de-ionized water. The samples were then moved into the plating bath for 20 minutes. For the preparation of the Cu-plated on FR4 substrates, a piece of FR4 coated in a thin layer of Cu was submerged in a sulfuric acid solution for 4 minutes with constant agitation. It was then washed with tap water and de-ionized water before it was submerged in the bath for plating.

3.3 Bath characteristics

Three electrolytes were used throughout the course of these experiments: Electroless bath type A and Electroless bath type B were used in the experiments that tested the effect of substrate roughness on H_2 incorporation. Electroless bath type C was used to test the effect of stabilizer on H_2 incorporation and the effect of surface potential on H_2 incorporation. These electrolytes were supplied by Atotech Deutschland GmbH. Electroless bath type A is an experimental bath, the other two are commercial baths. Electroless bath type C1, a representative commercial plating bath, contains 2g/l of Cu^{2+}, 0.4 g/l of Ni^{2+} (added via sulfate solutions), 3.5g/l HCHO as a reducing agent, 9 g/l of NAOH, 10.6 g/l of tartrate ions (added via potassium sodium tartrate) as well as an Atotech stabilizer solution whose makeup is proprietary. All these parameters

were kept constant, save for the potential on the surface of the substrate; it was either driven by an external battery or determined by solely bath chemistry. As in the other two baths, a magnetic stir bar and aeration were supplied to the bath at a constant rate to keep the bath uniform and prevent the reduction of Cu^{2+} to Cu^{+}. The makeup for Electroless bath type C is identical to Electroless bath type C1, but has different active components in the stabilizer system. Electroless bath type B and Electroless bath type A baths are slightly different from each other and Electroless bath type C.

3.4 Bath Maintenance

As each sample decreased some key bath components, intermittent monitoring of [HCHO], $[OH^{-}]$, and $[Cu^{2+}]$ was conducted to ensure that they were kept within the operational range specified by Atotech GmbH. These components were monitored through acid-base titrations and replenished using the stock chemicals from the bath makeup.

3.5 Measurement of hydrogen during plating

Hydrogen evolution during plating was measured with a non-invasive method similar to the one employed in [14]. An inverted plastic funnel, fused to a pipette, was placed in the bath. Underneath the funnel a custom-built holder for the sample was placed, which held the sample vertically in place during plating. This holder allowed the stir bar and the aeration to continue to mix the bath without interacting with the funnel apparatus. The air was then drawn out of the funnel and replaced with bath solution. When H_2 was emitted during plating, it would float up the pipette and displace the liquid at the top, and the corresponding drop in liquid volume was measured. A preliminary test of this setup illustrated that the gas entering the pipette from the

solution was minimal compared to the gas evolution observed during plating.

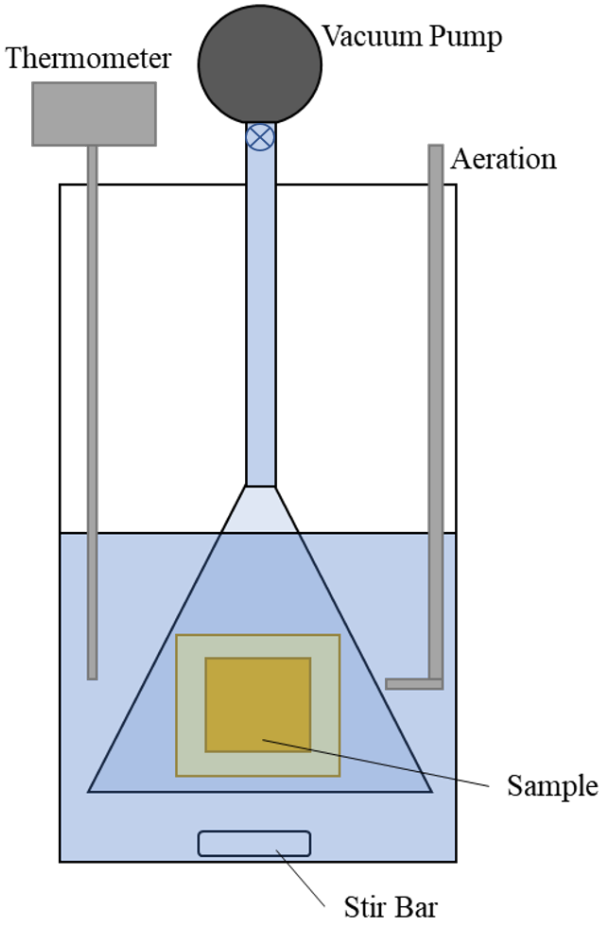

Figure 3.1: Schematic for the setup constructed to capture gas evolved during plating.

From this volume, we can calculate the moles of hydrogen by assuming that the hydrogen behaves as an ideal gas. After the sample is dried and weighed, the ratio between the moles of Cu plated and the moles of hydrogen released, x can then be calculated. [11]

$$x = \frac{2PV_f M_{Cu}}{RTm_{Cu}} \tag{3.1}$$

Where P is the ambient pressure, V_f is the volume of solution displaced, M_{Cu} is the molar mass of Cu, R is the gas constant, and T is the temperature of the bath, and m_{Cu} is the mass of Cu plated, as measured by mass gain.

3.6 Addition of stabilizer component

The order in which the reagents were added to the bath affected the bath's performance, and so careful attention had to be paid to the bath makeup to ensure the proper initial conditions were met. A stabilizer complex of Electroless bath type C, was removed completely from eleven samples, all plated on FR4 substrate. Two of these eleven were done at [Ni]=0ppm, two were done at [Ni]=800ppm. Additionally, six samples were run at [Ni]=0ppm and 100 % stabilizer, but the stabilizer was added after the HCHO, as it is normally added beforehand.

3.7 Measurement of hydrogen after plating

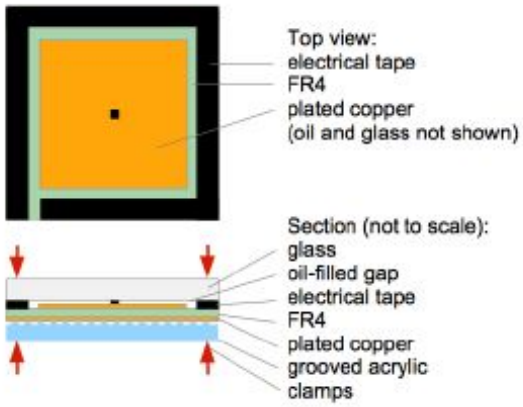

Figure 3.2: Schematic of device used to indirectly measure H_2 evolution after plating. Image reproduced from Sharma et al. (2018).

The sample, a piece of FR4 with a freshly plated Cu surface, is sandwiched between a glass window and a grooved acrylic plate. The distance between the glass and the Cu surface was determined by the thickness of the electrical tape. The tape thickness was chosen based on the expected amount of hydrogen gas evolved after plating. Gener-

ally, the tape thickness was either 70 microns or 150 microns. The space in-between was filled with Fisherbrand 19 Mechanical Pump Oil with blue N dye at 0.33% w/w to create an optical contrast against which we could measure hydrogen evolution after plating.

After the samples finished plating, they were removed from the bath, then rinsed with tap water and then deionized water. The samples were dried and placed on the acrylic plate. The Fisherbrand 19 Mechanical Pump Oil was added to the electroless Cu surface via a 1ml pipette. The amount added was on average 180 μl, but it varied slightly based on tape thickness. The pre-taped glass window was then pushed onto the sample, which formed a vacuum seal between the glass plate and the oil. The edges of the sample were clamped on four sides and then quickly cleaned, as oil would be pushed out of the small channel at the bottom during compression. Sometimes, small pockets of air would appear in the oil during this process, and it was recorded when they appeared. This process usually took between 2 to 3 minutes to complete. After this, the sample was moved to the analysis table where it was placed in an automated turnstile, and pictures were taken at a regular interval over 24 hours. The process of getting the sample from the bath to the taking of the first picture usually took between 5-8 minutes to complete.

3.8 Monitoring and controlling the mixed potential

The measurement of the open-circuit voltage between the plating surface and the bath was accomplished through a submerged Ag/AgCl reference electrode. A clamp was made from Cu wire and attached to the surface of the substrate, and the voltage was measured every second via an automated voltage measurement device throughout

the 20 minutes that the sample was in the bath. These measurements were taken on samples with both Cu and FR4 substrates, however when plating on FR4, there is lag in the measurement of surface voltage by roughly 1-2 minutes. This is due to the fact that FR4 is an insulator and the surface voltage could only be measured once a Cu seed layer had fully deposited on the surface.

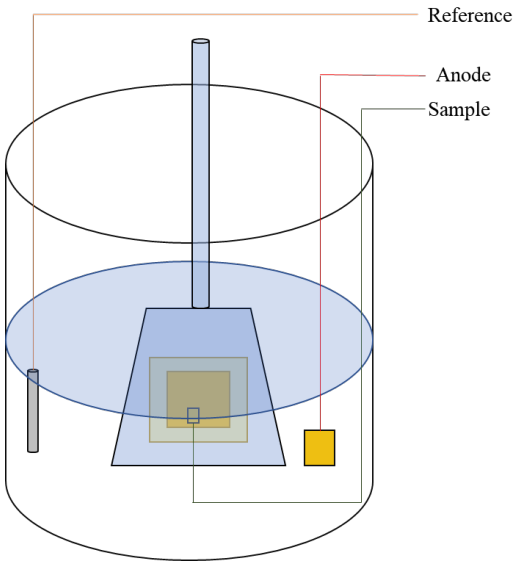

Figure 3.3: Electrical contacts into the bath. When the mixed potential was measured, the sample and reference electrodes were detached from the circuit in Figure 3.4. The thermometer and the aeration device are also present in the bath.

The measurement of the closed-circuit was a slightly more complicated process, though similar. To drive the surface potential to roughly -1.0V, the sample was connected to a circuit described by Figure 3.4. A 1.2 V battery powered the circuit, and a 47 Ω resistor was employed in series with a variable resistor to allow the user to control the surface potential of the sample with respect to the Ag/AgCl reference electrode. The variable resistor was generally kept around 100 Ω. A piece of Cu metal functioned as the anode for the circuit. A variable resistor was added to adjust the surface potential throughout 20 minutes of plating, as the mixed potential

of the sample typically increases during plating. [6] The reference and the sample were connected to an automated multimeter, which allowed the voltage between the reference electrode and the sample to be measured at constant intervals throughout the 20 minutes that the sample was immersed in the plating bath. The current to the sample, and the voltage between the sample and the anode were also measured. The most important measurement for this experiment was the voltage between the sample and the Ag/AgCl electrode.

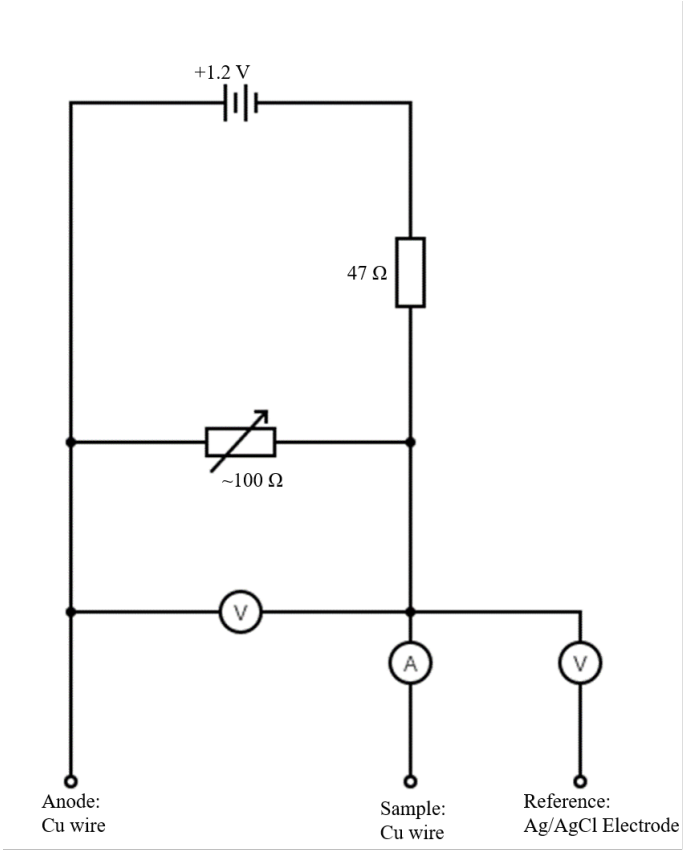

Figure 3.4: Schematic of the potentiostat. The variable resistor is denoted by the box with the diagonal arrow running through it.

3.9 Data Analysis

The hydrogen bubbles appear as Cu-colored spots in the blue oil film, which created a clear contrast that could be analyzed using the image analysis program FIJI. This program could measure the area covered by the bubbles on a 2D plane, which allowed us to quantify how much hydrogen was evolved during plating. First, the picture taken by the camera was cropped to only include the 'face' of the sample, only the area contained within the electric tape was analyzed. Then, all of the pictures from a given sample were turned into a black-and-white image. The area fraction, the ratio between the area of the picture and the area covered by hydrogen bubbles as a function of time, *f(t)*, was calculated from those FIJI data.

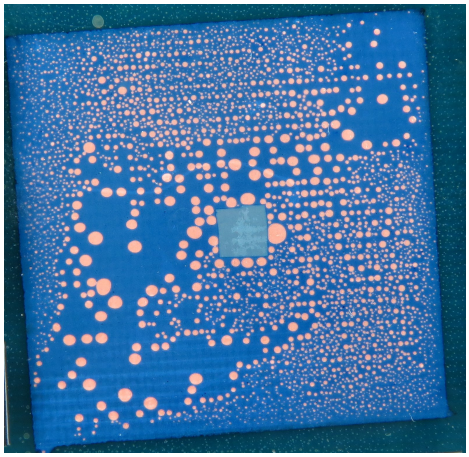

Figure 3.5: Picture of a sample close to the maximum area fraction. Notice the clear distinction between the Cu (light blue) and the FR4 (dark blue).

The calculation for the amount of hydrogen evolved after plating was simplified by assuming that the gas bubbles could be approximated as cylinders. This was a sensible approximation because the gap between the glass and the sample is on the order of a $10^2\mu$m while the average bubble had a diameter at roughly the same scale. Thus, the area of the average hydrogen bubble is roughly 100 times larger than the height,

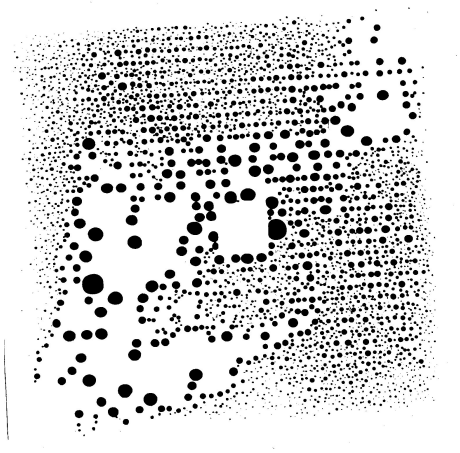

Figure 3.6: Image of sample after converting to black and white. This process creates a binary between area covered by H_2 and area that is not.

so any curvature in the vertical profile of the bubble does not contribute greatly to the volume. The average gas layer thickness is calculated as

$$\bar{h}(t) = \frac{f(t)hA}{A_{Cu}} \tag{3.2}$$

Where h is the thickness of the tape, A is the area bounded by the tape in the photograph, and A_{Cu} is the area within the Cu film in the photograph. When the glass was taped, it was ensured that there was enough room such that the Cu did not reach the edges of the tape during imaging, thus $A_{Cu} < A$. This was done to account for small fluctuations in the position of the hydrial in the tray. At the maximum value for $\bar{h}(t)$, the sample releases hydrogen at the same rate the device in Figure 3.3 loses hydrogen. It was also assumed that the hydrogen in the film at the end of plating is completely released when $\bar{h}(t)$ is at a maximum value. The consequence of this assumption being that any hydrogen left in the Cu film after this point is below or at the saturation point for Cu at room temperature. The ratio between moles of hydrogen released and moles of Cu plated, y, was calculated as

$$y = \frac{2\mathrm{PM}_{Cu}\max(\bar{h(t)})}{\mathrm{RT}h_f\rho_{Cu}} \tag{3.3}$$

Where h_f is the film thickness, ρ_{cu} is the density of Cu, M_{Cu} is the molar mass of Cu, R is the gas constant, and P and T are the ambient pressure and temperature, respectively.

Chapter 4

Results

4.1 The effect of surface roughness on hydrogen content

Cu on FR4 was plated on desmeared and non-desmeared faces of the substrate. This resulted in a difference in hydrogen incorporation into the Cu film itself, all else constant. These results support a claim from [2] that hydrogen congregates in pressurized voids that form inside the film. Plating does occur on smooth surfaces, but the Cu has a lower effective surface area to bind to, reducing the amount of Cu that is distributed onto the substrate.

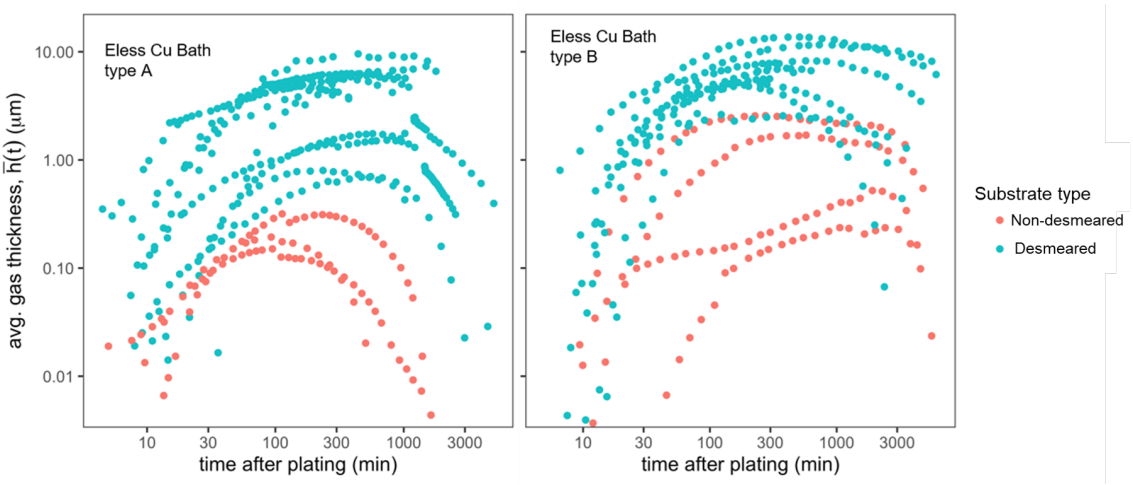

Figure 4.1: Average gas layer thickness, $\bar{h}$ over time for films prepared with Electroless bath type A and RA. Both desmeared and non-desmeared samples were tested. Non-desmeared data are represented in orange, desmeared data in teal.

The release of hydrogen takes about 10 times longer on the desmeared side compared to the non-desmeared side. This is believed to be a result of the film folding back onto itself during plating, which creates areas of high effective film thickness.

The hydrogen then takes longer to migrate through these areas of high thickness, which accounts for the increased time it takes for the gas to leave the sample.

4.1.1 Measuring hydrogen incorporation

When the data from Figure 4.1 is normalized to the amount of Cu plated onto the substrate, a contrast between the desmeared and non-desmeared samples is still seen. This difference is greater for samples prepared with Electroless bath type B than for Electroless bath type A. On the desmeared side, the amounts of incorporated hydrogen are around three times higher in Electroless bath type A and ten times higher in Electroless bath type B. We posit that there is little hydrogen contained in areas of the film with low effective thickness.

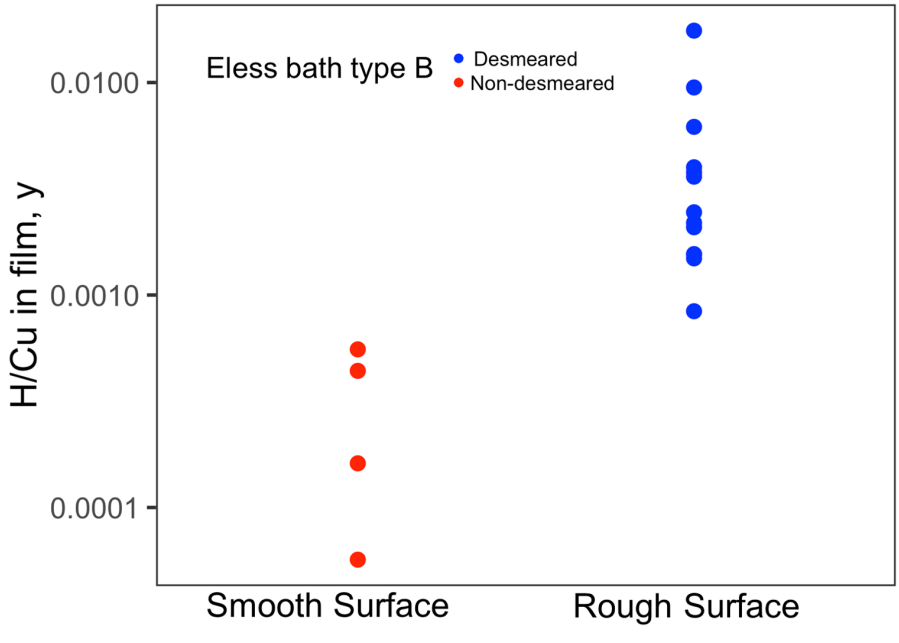

Figure 4.2: The ratio between deposited Cu and incorporated hydrogen by substrate roughness for Electroless bath type B bath.

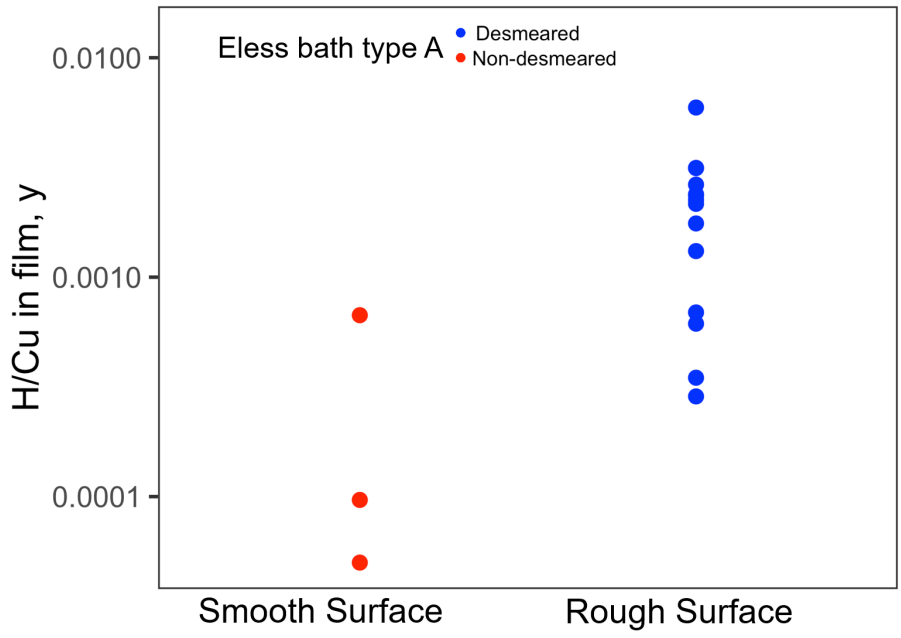

Figure 4.3: The ratio between deposited Cu and incorporated hydrogen by substrate roughness for Electroless bath type A bath.

4.2 Stabilizer effect on hydrogen incorporation

The stabilizer system, a proprietary mixture of chemicals, adheres to the substrate surface and reduces the effective plating area of Cu. [15] This process is known as surface poisoning. Sharma et. al in 2018 showed that Nickel mitigates surface poisoning, and increased nickel content results in decreased hydrogen incorporation. Stabilizer, through surface poisoning, also decreases the plating rate, though the addition of Ni to a stabilized bath increases the plating rate. [16] Our results showed that, when stabilizer is removed from the bath, hydrogen incorporation into the films is close to non-existent. These results suggest a fundamental role of the stabilizer, or an active component therein, in the incorporation of hydrogen into the Cu lattice during plating.

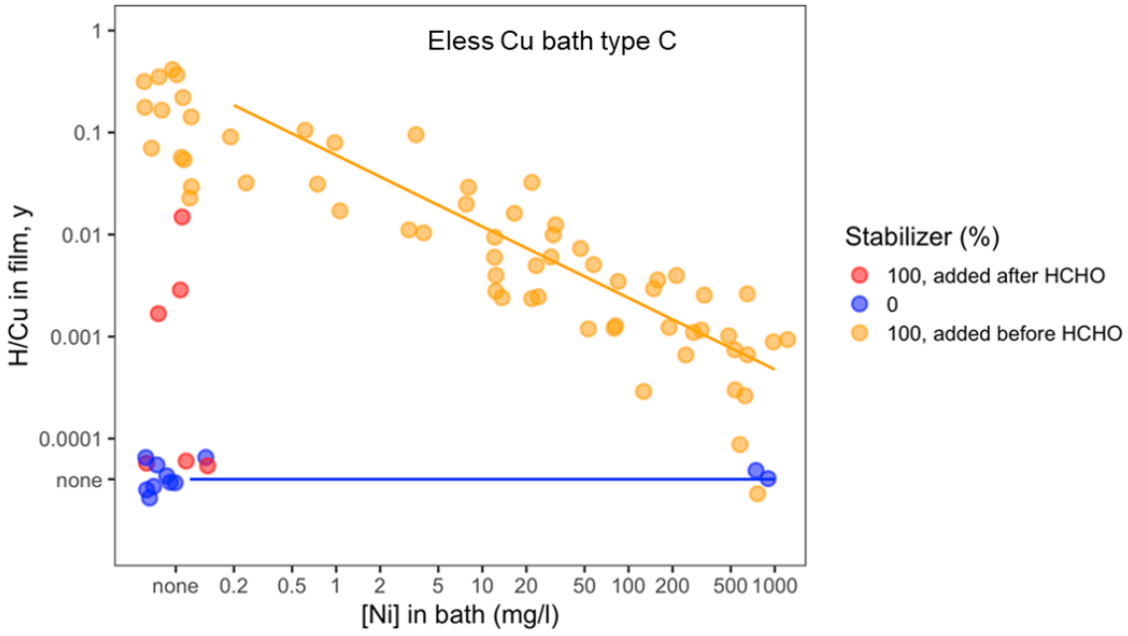

Figure 4.4: The ratio between deposited Cu and incorporated hydrogen as a function of Ni content in the bath. Further delineations are made between baths with and without stabilizer, and between baths where the stabilizer is added after the formaldehyde.

4.3 Stabilizer effect on hydrogen generation

In contrast to the results for the incorporated hydrogen y, the presence of stabilizer in the bath does not have a significant effect on the hydrogen evolved during plating. The surface poisoning, and the mechanism for hydrogen incorporation, does not appear to be involved in the generation of hydrogen during plating. There is a wide range for the amount of hydrogen generated, even with all other parameters held constant. Figure 4.5 contains the data illustrating these results. To begin measuring the evolved gas, the sample must be outfitted with the setup described in Figure 3.1 while plating. This process takes around 30 seconds. Additionally, the hydrogen does not immediately leave the surface during plating, the hydrogen bubbles must reach a critical volume before they float off the surface of the sample.

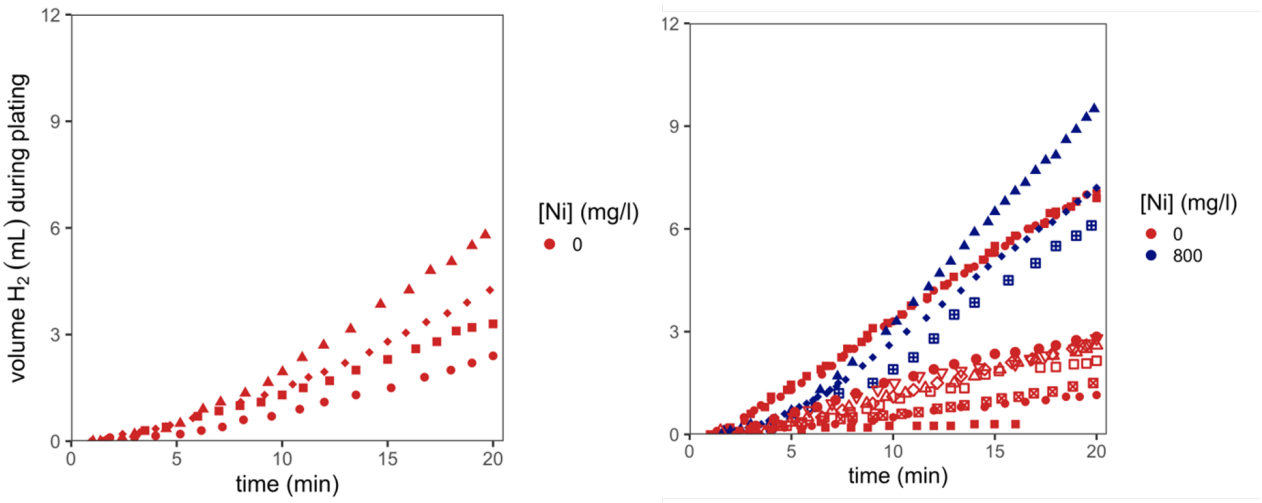

Figure 4.5: Volume of hydrogen evolved during plating for 100 % stabilizer and 0 % stabilizer in Elecroless bath type C. Notice the slight delay between starting the plating and the measurement of hydrogen.

4.4 Stabilizer decomposition with time

An important consideration for our data is the makeup of the active components of the stabilizer mixture, which is also referred to as a stabilizer system. Over time, an important active component decays with a half-life of roughly six months, which lowers hydrogen incorporation. This was known beforehand, and not discovered through our research. We were able to trace this degradation through our samples by selecting a range of samples, at [Ni]=0ppm, and the first data points starting in 2017. This trend further illuminated the role that the stabilizer plays in hydrogen incorporation in the sample. These results were obtained on both FR4 substrates and Cu-plated FR4 substrates.

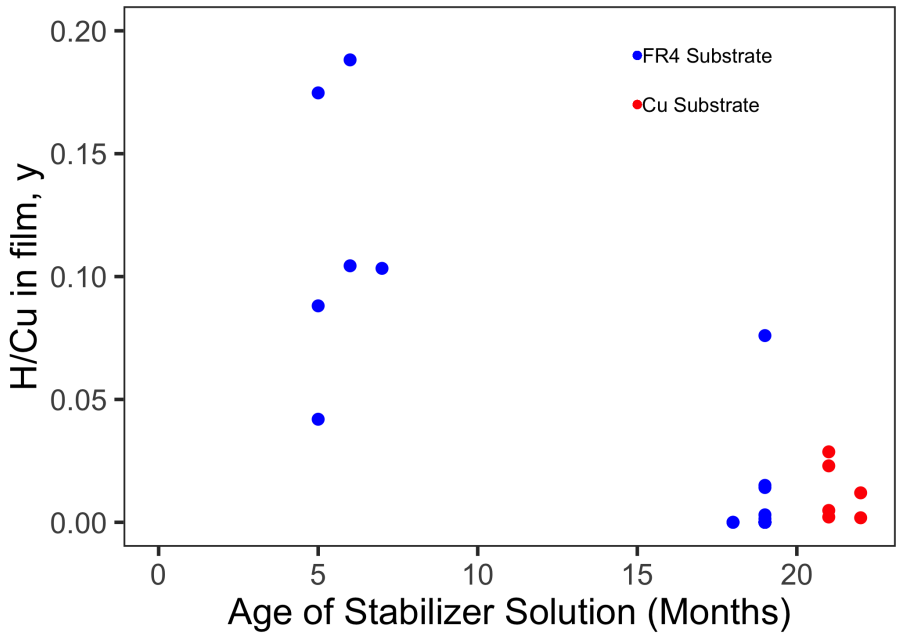

Figure 4.6: Volume of hydrogen evolved during plating for 100 % stabilizer solutions by volume. An active component degraded overtime, which reduced the poisoning of the surface by the stabilizer. Electrolyte: Electroless bath type C.

4.5 Simulating the Ni effect with a potentiostat

One of the effects of Ni in plating baths is a cathodic shift of the mixed potential of plating surface. The mixed potential, in the absence of Ni, hovers at around -0.8 V and decreases to about -0.7 V after 20 minutes of plating. In contrast, a bath at [Ni]=400 ppm stays at roughly -1.0 V. This effect is shown in Figure 4.7.

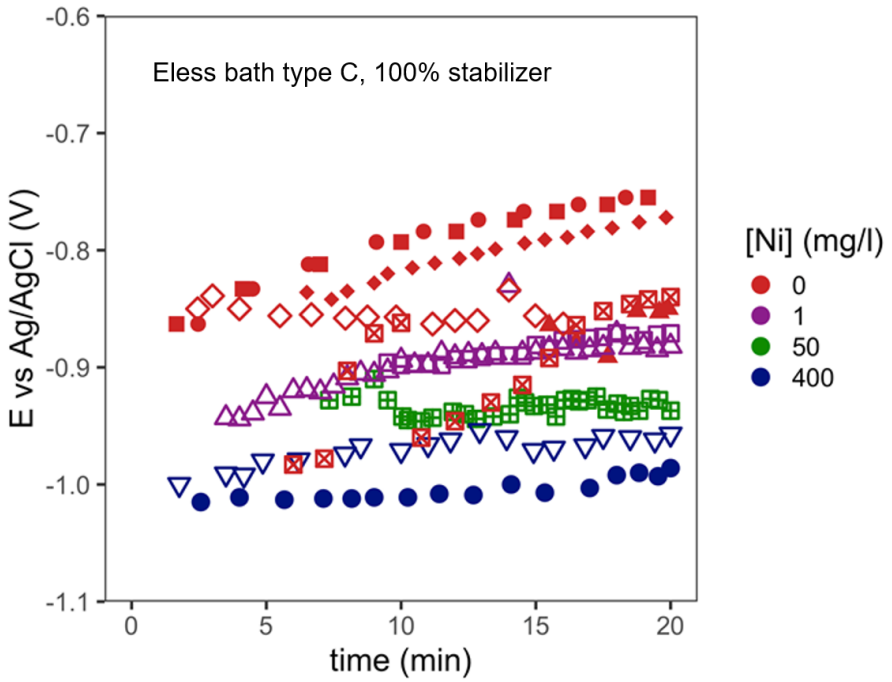

Figure 4.7: Open circuit potential of plating baths for Electroless bath type C. Notice that Ni produces a cathodic shift and also prevents the potential from becoming more positive as plating increases.

In an effort to better understand the mechanism by which Ni prevents the incorporation of hydrogen into the film, the mixed potential of the electroless plating process was overridden by a potentiostat, as described in Chapter 3. A 1.2 V battery was able to drive a voltage on the Cu substrate, which simulated the effect of Ni on the potential. The circuit performed well and was easy to disengage for open-circuit trials. Once engaged at the right setting, the potentiostat was able to keep the sample at a surface potential of -1.00 ± 0.02 V with small adjustments of the variable resistor on

the potentiostat shown in Figure 3.4.

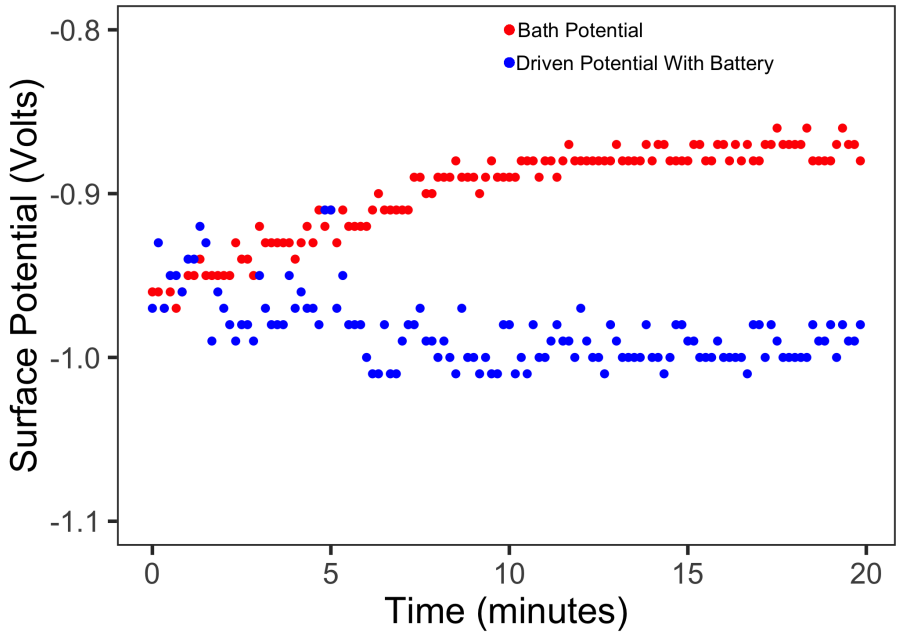

Figure 4.8: Potential for open circuit mixed potential vs controlled voltage trials done with a Cu substrate in a Electroless bath type C electrolyte. The initial fluctuations come from adjusting the variable resistor in order to attain a desirable voltage.

4.5.1 Potentiostat effect on hydrogen incorporation

The effect that the potentiostat had on the sample was significant, such that it could be discerned, even for the small number of trials that were conducted. The data in Figure 4.9 clearly illustrate that hydrogen incorporation is decreased by forcing the potential to -1.0 V throughout 20 minute plating period. While not proof that a decrease in the mixed potential decrease hydrogen incorporation, it provides a very clear next step in the research program. This evidence supports the thesis that the cathodic shift from Ni de-catalyzes the poisoning of the Cu film, and thus prevents hydrogen from being incorporated into the lattice. That is, the electric potential interacts with the stabilizer in such a way that it blocks or disrupts the adhesion of the stabilizer onto the substrate surface.

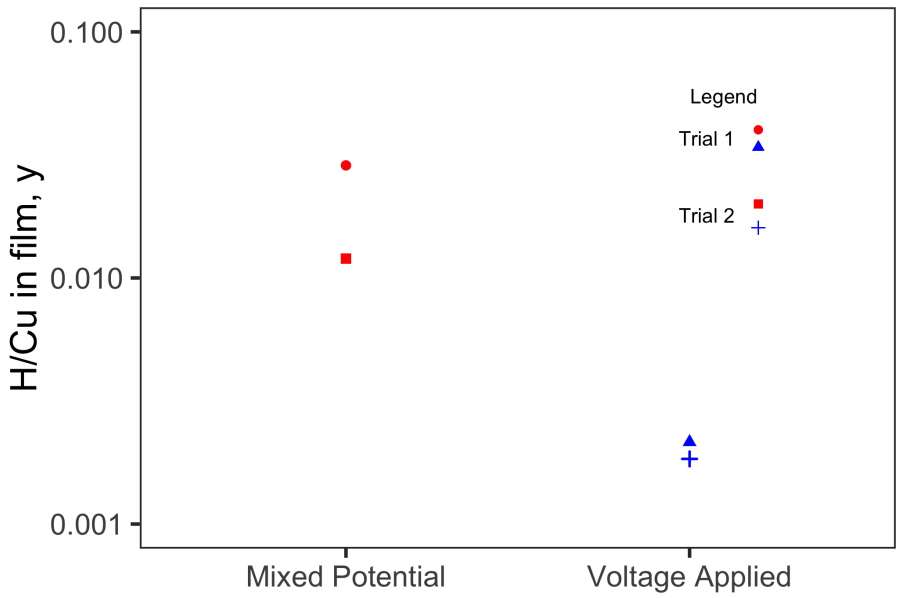

Figure 4.9: Potential for open circuit vs potentiostat driven (to -1.0 V) trials done a Cu-clad substrate in Electroless bath type C bath. The initial fluctuation comes from adjusting the variable resistor in order to attain a desirable voltage.

4.6 Effect of the stabilizer on the mixed potential

The stabilizer does not appear to impact the surface potential of the sample significantly. Figure 4.10 illustrates this point. Additionally, Ni in the bath results in a cathodic shift of the mixed potential even when stabilizer is not present. Thus, the cathodic shift that is produced by Ni is not simply a byproduct of its interaction with a component in the stabilizer.

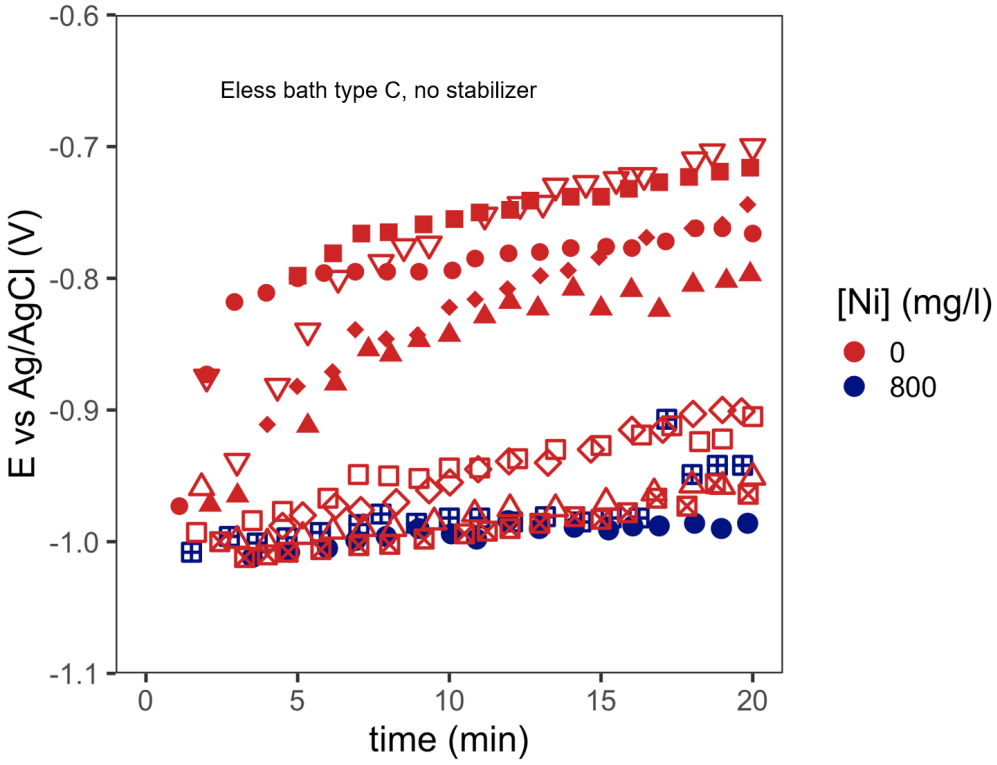

Figure 4.10: Mixed potential as a function of time. Notice both the wide range of potentials for baths without stabilizer and the effect that is produced when the bath is dosed up to [Ni]=800 ppm. Compare to Figure 4.7 for results with stabilizer added.

Chapter 5

Discussion

5.1 Substrate roughness and hydrogen incorporation

As was expected, increasing the substrate roughness through desmearing led to increased hydrogen incorporation, even when normalized to the amount of Cu plated onto the surface. Given desmearing the substrate roughly doubles the effective plating area of the substrate, the deposition of Cu to the FR4 is promoted, and the formation of the Cu film is accelerated. Interestingly, Electroless bath type A does not exhibit as significant a change in y, between desmeared and non-desmeared substrates, as Electroless bath type B. The differences between Electroless bath type B and Electroless bath type A in Figures 4.2 and 4.3 are difficult to reconcile, and more investigation is required to determine why one bath leads to a greater dependence on substrate roughness than the other.

This difference is made a bit more complicated by tracing the average gas layer thickness over time. While we see in Figure 4.1 that hydrogen incorporated into films on desmeared substrates in Electroless bath type B appears to take slightly longer to leave the film compared to P2, it is difficult to make an authoritative statement on the behaviour of either bath with respect to the diffusion rate after plating as there is significant scatter in the data.

Using Figure 5.1 as a reference, one can see the effect that substrate roughness has on the plating surface. As the Cu adheres to the surface, the film folds on top of itself, creating areas with high effective thickness. This folding process is not the primary

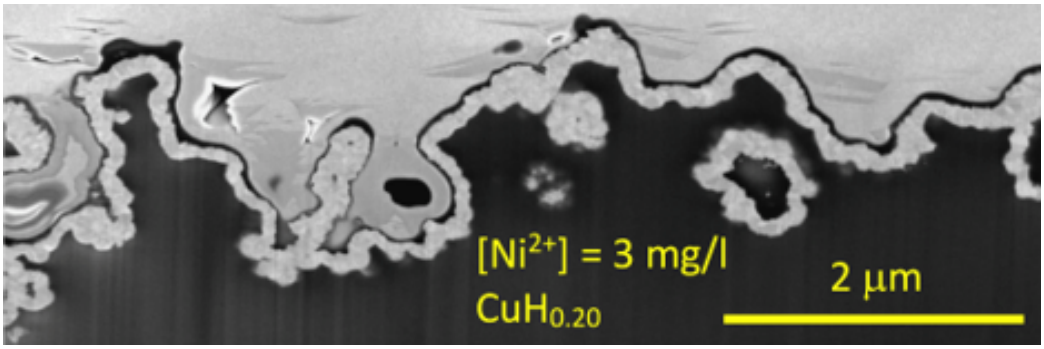

Figure 5.1: SEM micrograph with [Ni]=3mg/l and y=0.2. Notice how the roughness of the substrate promotes areas of the film with high thickness. Image via M. Balli, N. Baulke, and S. Heitz. Electrolyte: Electroless bath type C. Reproduced from Leger (2018).

cause of blistering, as any gas captured during this folding will not be at sufficiently high pressures to break through the film. Furthermore, it is known that hydrogen is at much higher equilibrium content inside the Cu than in the surrounding air at atmospheric pressure. [17] What the areas of high effective thickness do is promote the incorporation of atomic hydrogen into the lattice. [18] Then, as the hydrogen diffuses through the film, voids of highly pressurized hydrogen gas are formed under the surface. The depth of the film promotes the formation of voids as the hydrogen is unable to escape as easily compared to a flat surface.

5.2 Stabilizer's role in hydrogen incorporation

The stabilizer system poisons the surface, but its fundamental role is ensuring that Cu^{2+} ions do not reduce in the bath in to Cu^{+}, which leads to plating-out of Cu in the bulk of the bath, thereby destroying the metastable electrolyte in a spontaneous reaction. The data in Figure 4.4 indicates that the stabilizer is a fundamental mechanism for hydrogen incorporation in Cu films. The order in which the stabilizer and formaldehyde are added to the bath impacts the incorporation of hydrogen in the film. Looking again at Figure 4.4, we see that adding stabilizer after adding formaldehyde

to the bath decreases the amount of hydrogen incorporated into the film. .

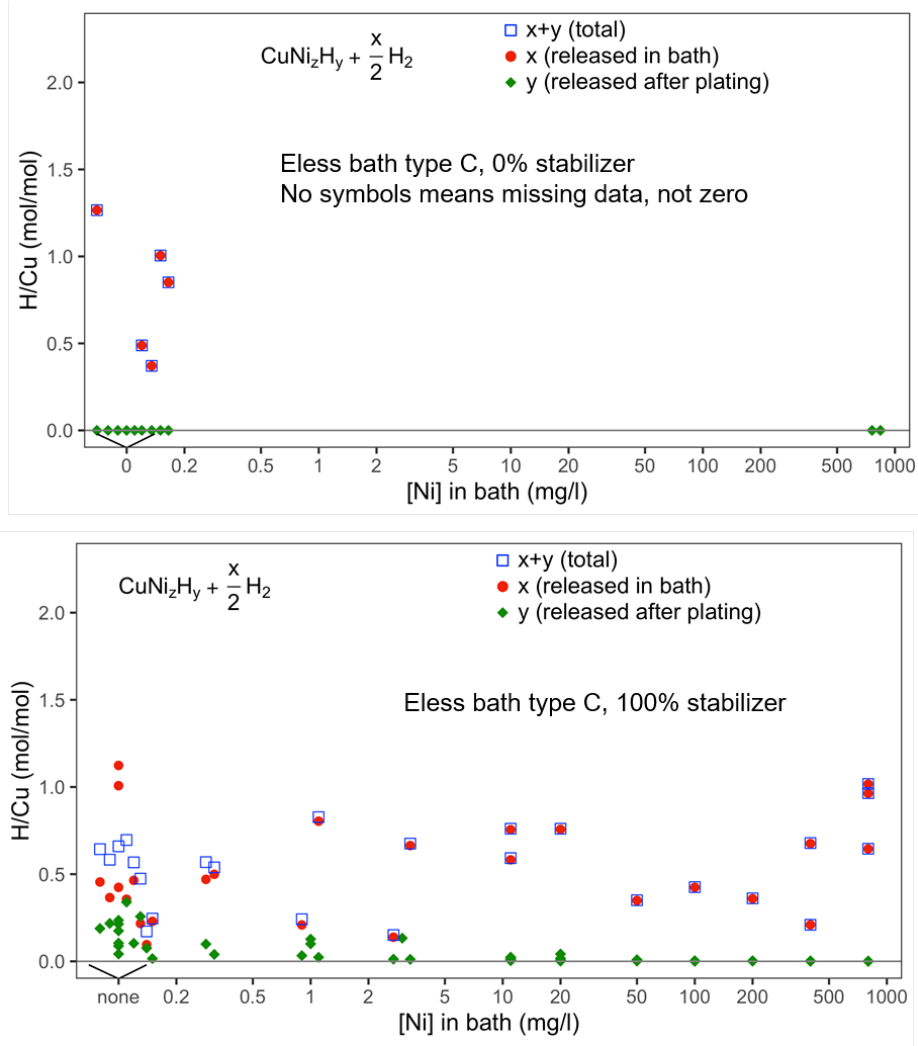

Figure 5.2: Total hydrogen gas production in Electroless bath type C baths at both 0 and 100 % stabilizer. Notice little change between the two charts in total gas released, as all the change comes from the suppression of y.

However, the decrease in incorporated hydrogen may also be due to the decay of the stabilizer system with time, and the large range of the data indicates that this could be investigated further to narrow down the causes of the decrease of hydrogen incorporation into the film. While hydrogen incorporation is suppressed, the total hydrogen evolved during plating is not changed by the presence of stabilizer. This is aligned with similar results regarding Ni concentration from [6] which shows that the hydrogen generated during plating is not correlated with the hydrogen incorporated during plating. Furthermore, the results fall within the established boundaries from Chapter 2, that is $0 \leq x + y \leq 2$

5.3 Potentiostat driven surface potential

To drive the surface potential to -1.0 V for the duration of plating, we had to first plate a thin layer of Cu over the entire FR4, creating a conducting substrate. While the process of utilizing an external current is antithetical to the concept of electroless plating, doing so allowed us to develop a better understanding of how Ni suppresses hydrogen incorporation into the Cu film. Due to time restraints, this experiment was not fully completed at the time of this writing, but it provides a promising next step for the research program. Our data suggest that by driving the surface potential of a conducting substrate in Electroless bath type C bath, one can simulate the effect that Ni has on the plating surface, thus hindering the incorporation of H_2 into the Cu film.

Component	[St.]=100 %	[St.]=0 %
[Ni] = 400 ppm	-1.0 V	-1.0 V
[Ni] = 0 ppm	-0.9 V to -0.8 V	-1.0 V to -0.7 V

Table 5.1: Mixed potential by component. Stabilizer does not have a discernible effect on the mixed potential, but there are variations in the data.

Moreover, one does not see an effect on the surface potential from the presence of

stabilizer. Though trials at [St.]= 0 % have a variety of mixed potentials, whose range encompasses that of stabilized baths. The data above in Table 5.1 illustrate that Ni has a pronounced effect on the mixed potential not only due to its cathodic shift, when [Ni] $\geq$ 400 ppm, there is a lack of time dependence on mixed potential. That is, the voltage is constant during plating.

5.4 Mixed potential and the stability of water

Recall Figure 2.1 and Reaction (2.6) in Chapter 2. There was a discussion of the relationship between pH and operational range of a standard electrolyte in Chapter 2. However, the relationship between potential was not explored, and this is where these results contribute more understanding. The cathodic shift produced by Ni, specifically that shift at [Ni]=400 ppm, is not accompanied by a decrease in plating rate or an increase in hydrogen generation through the suppression of Reaction (2.6). In fact, Logan et al. (2017) that the plating rate increases with Ni, and Sharma et al. (2018) showed that Ni does not increase hydrogen generation during plating. These findings are corroborated by Figure 5.2, where x+y is not significantly changed with the presence of Ni. More data is needed for non-stabilized baths at high [Ni] before any strong conclusions can be drawn from the data. However, there appears to exist a mechanism that, even when the bath undergoes a cathodic shift where water would be unstable, keeps Reaction (2.6) from being suppressed.

Chapter 6

Conclusion

A link between desmeared substrates and increased hydrogen incorporation was shown. Desmeared FR4 incorporated more atomic hydrogen per Cu plated compared to non-desmeared FR4, though this amount varied with electrolyte. Electroless bath type A saw a threefold increase in hydrogen incorporation while Electroless bath type B saw a tenfold increase in hydrogen incorporation. More work is needed to discern how to explain those differences. Additionally, it was found that hydrogen evolution post-plating takes roughly 10 times longer to on the desmeared side of the FR4 substrate compared to the non-desmeared side. This indicates that there is significant hydrogen incorporation in areas where the film is thicker, as the hydrogen takes more time to work its way through the film. Further work on this subject could involve quantifying the relationship between average film thickness and hydrogen incorporation.

Additionally, a method for controlling the surface potential of a substrate through a potentiostat was implemented. This method was able to simulate the cathodic shift produced by the presence Ni, as well as keep the voltage constant during plating. This method is limited to metal substrates, though early results suggest that the mixed potential of the plating surface has a significant effect on hydrogen incorporation. Implementing the cathodic shift (that is usually obtained by adding Ni) with a potentiostat leads to the same reduction in hydrogen uptake by the sample.

The stabilizer system, in Electroless bath type C baths, was shown to be a fundamental driver of hydrogen incorporation into electroless Cu films. Without the presence of stabilizer, the incorporated hydrogen in Cu films drops to zero. However, the pres-

ence of stabilizer does not impact the generation of hydrogen during plating. This results indicates that Ni encourages the de-poisoning of the substrate surface, hence removing the stabilizer complex and the source of hydrogen incorporation. However, more investigation is needed to determine how the stabilizer system promotes the incorporation of hydrogen into Cu films.

References

[1] J. E. Graebner and Y. Okinaka, Journal of Applied Physics **60**, 5 (1986).

[2] S. Nakahara, Acta Metallurgica **36**, 13 (1988).

[3] J.-W. Seo et al., Korean Journal of Chemical Engineering **29**, 5 (2012).

[4] Y. Okinaka and H. K. Straschil, Journal of the Electrochemical Society **133**, 8 (1986).

[5] S. Bamberg et al., Thin Solid Films **520**, 7 (2012).

[6] T. Sharma et al., Thin Solid Films **666**, 9 (2018).

[7] E. Logan, *Surface Kinetics in Electroless Copper Plating*, Undergraduate Thesis, Mount Allison University (2016).

[8] M. Enyo, Journal of Electroanalytical Chemistry **201**, 13 (1986).

[9] M. Paunovic, *Modern Electroplating*, John Wiley & Sons, INC., Hoboken (2010).

[10] J. E. A. M. van den Meerakker and J. W. G. de Bakker, Journal of Applied Electrochemistry **20**, 6 (1990).

[11] A. Leger, *Hydrogen Effusion From Electroless Copper Deposits*, Undergraduate Thesis, Mount Allison University (2018).

[12] P. Bindra and J. R. White, *Electroless Plating: Fundamentals and Applications*, American Electroplaters and Surface Finishers Society, Orlando (1990).

[13] T. Sharma et al., Microelectric Engineering **140**, 9 (2015).

[14] T. Bernhard, Journal of Microelectronics and Electronic Packaging **12**, 6 (1990).

[15] J. Li and P. Kohl, Journal of the Electrochemical Society **150**, 5 (2003).

[16] E. Logan et al., Thin solid films **626**, 9 (2017).

[17] H. Magnusson and K. Frisk, Journal of Phase Equilibria and Diffusion **38**, 5 (2017).

[18] H.C.Rogers, Science **159**, 8 (1968).